Applied Catalysis B: Environmental 84 (2008) 268–276

Contents lists available at ScienceDirect

Applied Catalysis B: Environmental

journal homepage: www.elsevier.com/locate/apcatb

Regenerable ceria-based SO_x traps for sulfur removal in lean exhausts

Lisa Kylhammar *, Per-Anders Carlsson, Hanna Härelind Ingelsten, Henrik Grönbeck, Magnus Skoglundh

Competence Centre for Catalysis, Chalmers University of Technology, SE-412 96 Göteborg, Sweden

ARTICLE INFO

Article history:
Received 18 December 2007
Received in revised form 30 March 2008
Accepted 5 April 2008
Available online 11 April 2008

Keywords:
FTIR spectroscopy
Storage mechanism
CeO_2
Pt
Sulfur oxide

ABSTRACT

Bare and Pt-containing CeO_2, Al_2O_3:MgO mixed oxide and Al_2O_3 have been investigated as potential regenerable sulfur oxides (SO_x) traps. The samples were evaluated by lean SO_x adsorption and temperature programmed desorption using synthetic gas compositions. In addition, combined DRIFT spectroscopy and mass spectrometry were employed to obtain mechanistic information on the adsorption of SO_x. The results suggest Pt/CeO_2 as promising SO_x trap material owing to a high storage capacity at 250 °C in combination with efficient release above 600 °C. The presence of Pt is generally found to enhance the lean SO_x storage capacity at 250 °C for CeO_2-based samples. Lean SO_2 adsorption on CeO_2 is found to proceed via the formation of surface and bulk sulfates, where the latter is formed more rapidly for the Pt-containing CeO_2 sample. Ceria samples pre-exposed to high amounts of SO_2 at 250 and 400 °C show lower SO_x storage capacity and higher SO_x release as compared to fresh samples. This indicates that under the conditions used in this study, a part of the storage sites on CeO_2 are non-regenerable.

1. Introduction

One strategy to reduce CO_2 emissions within the transportation sector is to increase the fuel efficiency by the use of lean-burn or diesel engines [1]. The lean character of the exhausts from these engines requires other aftertreatment concepts than standard three-way technology. One such concept is NO_x storage catalysis which has shown promising characteristics for NO_x reduction under net-lean conditions [2]. This concept is based on temporary storage of NO_x on basic storage sites, usually provided by metal oxides like barium oxide (BaO), during lean periods and release with subsequent reduction of NO_x over noble metals during short periods of rich or stoichiometric conditions. However, one issue regarding this type of catalyst is the sensitivity of the storage material to sulfur, i.e., high affinity towards storage of sulfur oxides (SO_x) under lean conditions and negligible release of sulfur compounds under the NO_x regeneration phase. In course of time, a progressing sulfur poisoning will reduce the NO_x storage capacity and the number of available NO_x storage sites will eventually become critically low, which leads to insufficient NO_x storage and reduction [2–5]. To regenerate the NO_x storage capacity at this stage, thermal decomposition under net reducing conditions by a drastic increase of temperature is essentially the only solution. However, the temperature required for this procedure is too high to guarantee the stability of the catalyst towards thermal deactivation.

Sulfur containing species in the exhausts originate from fuel and lubricants. Even though the content of sulfur in the fuel has been significantly reduced over the years, the presence of sulfur will always lead to reduced NO_x storage capacity. Thus, within the present technology, strategies to handle sulfur in the exhaust are necessary. This can be achieved by increasing the sulfur tolerance of the aftertreatment system or preventing SO_x from reaching the NO_x storage catalyst by using upstream SO_x traps. The sulfur tolerance of the catalyst can be increased by enhancing the release of sulfur species during regeneration and/or by decreasing the sulfur affinity of the storage material. The sulfur release during regeneration can, for example, be facilitated by using thinner washcoat layers [6] or by adding TiO_2 to the Al_2O_3-support of the NO_x storage catalyst [1]. Moreover, the amount of sulfur adsorbed can be decreased by replacing the NO_x storing component with a material with lower affinity towards sulfur compounds [7,8]. A few different SO_x trap strategies have been suggested and materials such as BaO supported on Al_2O_3 [9], Ba/Cu–benzene tricarboxylate [10], $K_xMn_8O_{16}$ [11] and MnO [12] have been proposed as SO_x adsorbents.

In the present work, a series of different materials is evaluated as regenerable SO_x traps. Such traps should, in different temperature intervals, store and release SO_x under lean conditions. During regeneration of the SO_x trap, the exhausts will be by-passed

* Corresponding author. Tel.: +46 31 772 29 59; fax: +46 31 16 00 62.
E-mail address: lisa.kylhammar@chalmers.se (L. Kylhammar).

0926-3373/$ – see front matter © 2008 Elsevier B.V. All rights reserved.
doi:10.1016/j.apcatb.2008.04.003

the NO_x storage catalyst to minimize the sulfur exposure. This strategy should be chosen as sulfur species previously have been reported to adsorb on the catalyst under both lean and rich conditions blocking storage and noble metal sites [13]. To our knowledge, this regeneration technique has not previously been suggested in the literature. The desired properties of the SO_x adsorbent are to store SO_x under normal lean exhaust conditions in the temperature interval 200–500 °C and release the stored sulfur species under lean conditions at temperatures slightly above 500 °C. In this way, the fuel consumption required to produce the heat for regeneration is minimized. To avoid permanent sulfur poisoning, we intuitively choose to compare different metal oxides that are sufficiently basic to store SO_x, e.g. CeO_2, Al_2O_3:MgO mixed oxide and Al_2O_3, but less basic than BaO. Ceria is an interesting oxide for many aftertreatment applications. For example, ceria is used as an oxygen storage component in the three-way catalyst and as SO_x traps for stationary applications [14]. It is known that sulfates may form on ceria upon exposure to SO_2 even in the absence of oxygen [15], a property that probably is caused by the high oxygen mobility within the material. Adsorbents based on Al_2O_3:MgO mixed oxides from hydrotalcite precursors have also been suggested as SO_x traps for stationary applications [16]. By using hydrotalcite precursors for the mixed oxide, it is possible to control the basicity of the storage material by varying the Al_2O_3:MgO ratio. Alumina, which is an amphotheric oxide, is the least basic oxide in the present study and is included primarily as reference material. Boehmite is used as binder for the monolith samples which means that all samples contain some Al_2O_3. To investigate the suitability of these metal oxides as SO_x traps, we have employed both kinetic studies in a flow-reactor and mechanistic studies by combined qualitative diffuse reflectance infrared fourier transformed spectroscopy (DRIFTS) and mass spectrometry. The influence of noble metal on the SO_x storage and release properties of the SO_x traps is investigated as well as the stability of the SO_x adsorbent.

2. Experimental considerations

2.1. Sample preparation and characterisation

The metal oxides used as SO_x adsorbents were; CeO_2 (99.5 H.S.A. 514, Rhône-Poulenc), Al_2O_3:MgO (30:70 wt.%) mixed oxide prepared from a hydrotalcite precursor (Condea) and Al_2O_3 (Puralox SBa-200, Sasol). All samples were pre-treated in air at 750 °C for 2 h. The Pt-containing powder samples were prepared by wet impregnation of Al_2O_3 and CeO_2 using $Pt(NO_3)_2$ (Hereaus) as precursor. Due to different point of zero charge for the oxides, the impregnation was performed at pH 2 and 3 for the Al_2O_3 and CeO_2 sample, respectively. After impregnation, the slurries were instantly frozen with liquid nitrogen and freeze-dried. The resulting powder samples were finally calcined in air at 600 °C for 1 h (heating rate of 4.8 °C/min from 25 to 600 °C). Surface area measurements of the powder samples were performed by N_2-physisorption at 77 K using a Micromeritrics Tristar instrument. For a few selected samples, the specific surface areas, calculated using the BET-method [17], are summarised in Table 1.

Monoliths samples (Ø = 20 mm and length = 20 mm) were cut from a commercial honeycomb cordierite structure with 400 cpsi. The monoliths were coated with the SO_x adsorbent material following the procedure described in Ref. [18]. As a binder for the adsorbent material, Boehmite (Disperal SOL P2, Condea) was used in all samples (20 wt.% of the dry material in the slurry). After coating, all monolith samples were calcined in air at 650 °C for 3 h. The Pt-containing samples were prepared by impregnation of the coated monoliths using $Pt(NO_3)_2$ as platinum precursor for the Al_2O_3 and CeO_2 samples and $Pt(NH_3)_2(NO_2)_2$ (Johnson Matthey) for the Al_2O_3:MgO sample. The impregnation was performed at pH 2, 3 and 8 for the Al_2O_3, CeO_2 and Al_2O_3:MgO sample, respectively. After impregnation, the monolith samples were dried in air at 80 °C for 12 h. The temperature was thereafter gently increased by 4.3 °C/min to 600 °C and the samples were finally calcined in air at this temperature for 1 h.

Table 1
Specific surface area of Al_2O_3 and CeO_2-based powder samples

Sample	Specific surface area (m^2/g)	Comment
CeO_2	254	Fresh
CeO_2	82	Air, 750 °C, 2 h
5 wt.% Pt/CeO_2	78	CeO_2 treated in air, 750 °C, 2 h and impregnated with Pt
Al_2O_3	203	Fresh
Al_2O_3	187	Air, 750 °C, 2.5 h
5 wt.% Pt/Al_2O_3	174	Al_2O_3 treated in air, 750 °C, 2.5 h and impregnated with Pt

2.2. Isothermal SO_2 adsorption followed by temperature programmed desorption

The flow-reactor experiments with monolith samples were performed using a quartz tube reactor equipped with a gas mixer unit (Environmentics 2000) for control of the inlet gas composition, and a surrounding metal coil for resistive heating of the reactor tube. A thermocouple (type K, Pentronic) placed 10 mm upstream of the monolith was used together with a Eurotherm regulator to control the inlet gas temperature. A second thermocouple was positioned inside the monolith, about 2 mm from the end of the sample, to measure the sample temperature. To facilitate the analysis of the total SO_x outlet concentration, the experimental method previously reported by McLaughlin et al. [19] was used. Following this method, the outlet gas flow was first passed over an oxidation catalyst before introduced to the SO_2 analyser (non-dispersive IR, Maihak UNOR 610). For further information about the experimental method see Appendix A.

For all experiments, the total flow was 3500 ml/min, which corresponds to GHSV = 33 400 h^{-1}, and Ar was used as balance. Prior to each experiment, the samples were treated in 7% O_2 for 10 min at 500 °C. The temperature was thereafter decreased and lean SO_x adsorption was performed (100 ppm SO_2 and 7% O_2 in Ar) at 250 or 400 °C for 1 h. The high SO_2 concentration in these experiments was used to assure measurement accuracy rather than mimicking real lean exhaust conditions. After the SO_2 exposure, temperature programmed desorption (lean SO_x-TPD) was performed by increasing the temperature by 10 °C/min to 700 °C in 7% O_2. The temperature was kept constant at 700 °C for 20 min before cooling in Ar.

2.3. DRIFT spectroscopy measurements

FTIR measurements were performed with powder samples in diffuse reflectance mode using a Bio-Rad FTS6000 spectrometer equipped with a Harrick Praying Mantis DRIFTS cell and a MCT detector. The resolution was 1 cm^{-1} and the number of scans per spectrum was set to 20. All experiments were performed with fresh samples using a total gas flow of 100 ml/min and Ar as balance. Prior to each experiment, the sample was treated in 20% O_2 at 500 °C for 10 min followed by cooling in 7% O_2 to the temperature to be studied, i.e., 250 or 400 °C. Because the windows in the reactor dome absorb IR radiation in the same wavenumber

Table 2
Procedure during DRIFTS experiments

Step	Time (min)	Gas feed (Ar as balance)	Dome on/off	Comment
1	5	7% O_2	On	
2	3	7% O_2	Off	Spectra recorded before SO_2 exposure
3	5	7% O_2	On	
4	5	300 ppm SO_2 and 7% O_2	On	
5	15	7% O_2	On	
6	3	7% O_2	Off	Spectra recorded after 5 min of SO_2 exposure
7	3	7% O_2	On	
8	5	300 ppm SO_2 and 7% O_2	On	
9	15	7% O_2	On	
10	3	7% O_2	Off	Spectra recorded after 10 min of SO_2 exposure
11	3	7% O_2	On	
12	10	300 ppm SO_2 and 7% O_2	On	
13	15	7% O_2	On	
14	3	7% O_2	Off	Spectra recorded after 20 min of SO_2 exposure
15	3	7% O_2	On	
16	20	300 ppm SO_2 and 7% O_2	On	
17	15	7% O_2	On	
18	3	7% O_2	Off	Spectra recorded after 40 min of SO_2 exposure
19	3	7% O_2	On	
20	20	300 ppm SO_2 and 7% O_2	On	
21	15	7% O_2	On	
22	3	7% O_2	Off	Spectra recorded after 1 h of SO_2 exposure
23	3	7% O_2	On	
24	120	300 ppm SO_2 and 7% O_2	On	
25	15	7% O_2	On	
26	3	7% O_2	Off	Spectra recorded after 3 h of SO_2 exposure

region as some sulfur species, the dome was removed during the recording of spectra. To manage this procedure while simultaneously facilitate the study of how different species are formed on the samples, the SO_x adsorption experiments were performed as a sequence of several steps described in Table 2. During SO_2 exposure and subsequent flushing of the reaction cell, the dome was attached to the cell. After flushing, the dome was removed for 3 min and the spectra were recorded under continuous flushing of 7% O_2 in Ar at the adsorption temperature. By this procedure, sample exposure to air is minimized which also was confirmed by reference experiments without SO_2 exposure showing no detectable IR bands from species that possibly can originate from air contaminants.

3. Results

3.1. Flow-reactor experiments

Fig. 1 shows the outlet SO_x concentrations during lean SO_x adsorption for the series of monolith samples (CeO_2, Al_2O_3:MgO, Pt/Al_2O_3, Pt/CeO_2 and Pt/Al_2O_3:MgO) at 250 °C. Repeated lean SO_x adsorption at 250 °C followed by TPD experiments were performed and the results from the 7th cycle are displayed. As a reference, also the results for the corresponding experiments with empty reactor are included in the figure. With the assumption that the amount of SO_x not reaching the detector is adsorbed on the sample, the area between the SO_x signal for the empty reactor and the actual experiment in Fig. 1 is proportional to the SO_x storage capacity. At $t = 1$ min, 100 ppm SO_2 is introduced which results in a rapid increase of the SO_x outlet concentration. After the initial phase, a twitch on the SO_x signal to a slower increase in outlet SO_x concentration can be seen for all samples. After the twitch, the most rapid increase is observed for the Al_2O_3:MgO-based samples and throughout the experiment the SO_x signal for the Al_2O_3:MgO-based samples declines and levels out close to the feed gas concentration around $t = 30$ min. Compared to the Al_2O_3:MgO-based samples, the SO_x signal for the CeO_2 sample increases somewhat slower after the twitch and the SO_x concentration levels out close to the feed gas concentration around $t = 40$ min. In the case of the Pt/CeO_2 and Pt/Al_2O_3 samples, however, the characteristic of the SO_x signal is different. The twitch to a slower increase of the outlet SO_x concentration after the initial phase is significantly more pronounced and a second twitch appears around $t = 10$ and 12 min for the Pt/Al_2O_3 and Pt/CeO_2 samples, respectively. Thereafter, the increase in SO_x concentration then declines for both samples although the SO_x concentration never reaches the feed gas level during the experimental time (60 min).

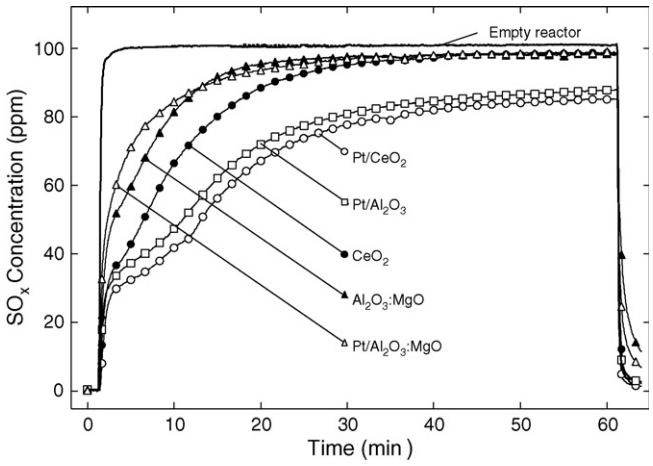

Fig. 1. SO_x signals during SO_2 adsorption at 250 °C for CeO_2, Al_2O_3:MgO (30:70), Pt/Al_2O_3, Pt/CeO_2 and Pt/Al_2O_3:MgO samples. The response for the empty reactor is included as system reference. Active mass: 0.87 g/monolith sample. Feed composition during adsorption: 100 ppm SO_2 and 7% O_2 in Ar. GHSV: 33 400 h^{-1}.

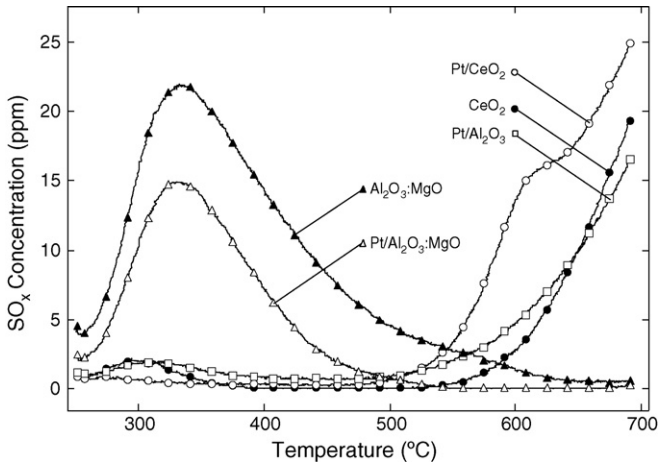

Fig. 2. Lean SO_x-TPD results for the CeO_2, Al_2O_3:MgO (30:70), Pt/Al_2O_3, Pt/CeO_2 and Pt/Al_2O_3:MgO samples after SO_2 adsorption at 250 °C. Feed composition during the TPD: 7% O_2 in Ar. GHSV: 33 400 h^{-1}. Ramp rate: 10 °C/min.

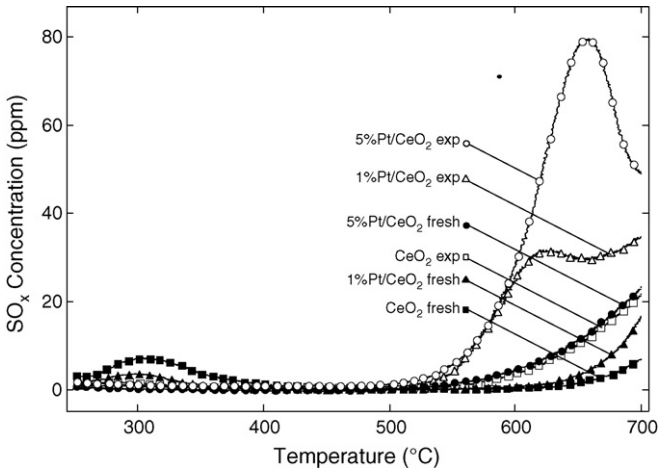

Fig. 4. Lean SO_x-TPD results for fresh and SO_2 pre-exposed CeO_2-based samples containing 0, 1 and 5 wt.% Pt, respectively after SO_2 adsorption at 250 °C. Feed composition during the TPD: 7% O_2 in Ar. GHSV: 33 400 h^{-1}. Ramp rate: 10 °C/min.

The results from the subsequent lean SO_x-TPD experiments are displayed in Fig. 2. For the Al_2O_3:MgO containing samples, SO_x desorption starts already at 260 °C and clear maxima are observed around 330 °C. No significant SO_x desorption is observed above 550 and 650 °C for the Pt/Al_2O_3:MgO and Al_2O_3:MgO samples, respectively. Except for minor desorption around 300 °C, no substantial SO_x desorption is detected below 500 °C for the Al_2O_3 and CeO_2-based samples. Instead, SO_x desorption starts at temperatures slightly above 500 °C and increases rapidly at about 550 °C, especially for the Pt/CeO_2 sample. A special feature for the Pt/CeO_2 sample is the well-pronounced shoulder on the SO_x signal at around 600 °C. The Pt/Al_2O_3, Pt/CeO_2 and CeO_2 samples all show the highest desorption at 700 °C which is the maximum temperature during the experiment.

The lean SO_x storage and TPD results indicate that Pt/CeO_2 is a promising SO_x trap material and that the presence of Pt significantly influences the performance of CeO_2-based SO_x traps. Therefore, further studies were performed to investigate the SO_x adsorption and regeneration properties of CeO_2-based SO_x traps containing 0, 1 and 5 wt.% Pt. Figs. 3 and 4 show the results from the lean SO_x adsorption and subsequent SO_x-TPD experiments (analogous to Figs. 1 and 2) for both fresh and SO_2 pre-exposed CeO_2-based samples. With SO_2 pre-exposed samples we refer to samples that in addition to the lean SO_x adsorption and TPD experiments have been exposed to 700 ppm SO_2 and 7% O_2 in Ar for 1 h first at 250 °C and then for 1 h at 400 °C. In order to remove SO_x from regenerable sites, a TPD is perfomed before starting the second lean SO_x adsorption and TPD experiment with the pre-exposed sample. During the SO_x adsorption (cf. Fig. 3), all samples have similar uptake performance as the CeO_2 samples in Fig. 1. For the fresh samples the outlet SO_x concentration is generally lower during 1 h of lean SO_2 exposure for samples with higher Pt loading. The same trend is observed for the SO_2 pre-exposed samples. Comparing fresh and SO_2 pre-exposed samples with the same Pt loading reveal that the outlet SO_x concentration is generally lower for the fresh samples. The only exception is the 5 wt.% Pt/CeO_2 sample where the difference between fresh and SO_2 pre-exposed samples is very small. Considering the lean SO_x-TPD, a small amount of SO_x desorbs already around 300 °C from the fresh 0 and 1 wt.% Pt/CeO_2 samples. Desorption at this low temperature is neither observed for the 5 wt.% Pt/CeO_2 sample nor for the pre-exposed samples. For the fresh samples, increased SO_x desorption

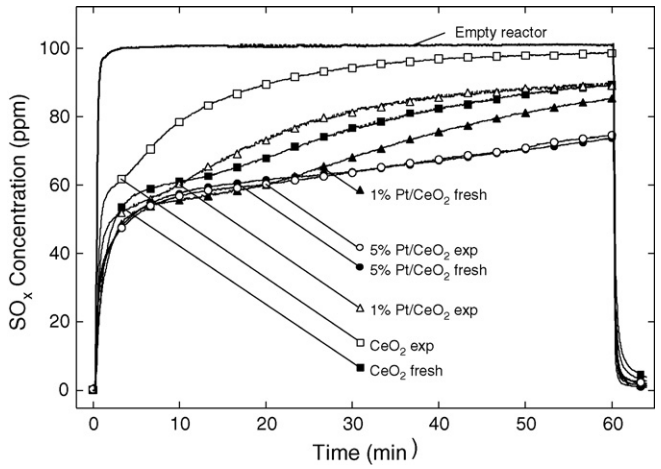

Fig. 3. SO_x signals during SO_2 adsorption at 250 °C for fresh and SO_2 pre-exposed CeO_2-based samples containing 0, 1 and 5 wt.% Pt, respectively. The response for the empty reactor is included as system reference. Active mass: 1.00 g/monolith sample. Feed composition during adsorption: 100 ppm SO_2 and 7% O_2 in Ar. GHSV: 33 400 h^{-1}.

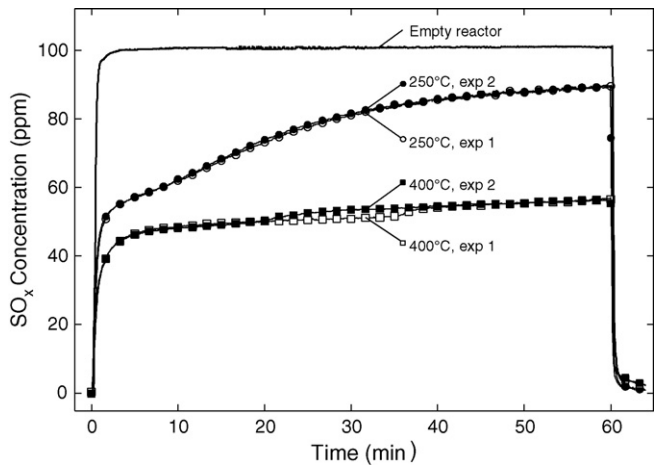

Fig. 5. SO_x signals during lean SO_2 adsorption for repeated experiments for a 1 wt.% Pt/CeO_2 sample. The SO_2 adsorption temperature was alternated in the following sequence: 400, 250, 400 and 250 °C. The response for the empty reactor is included as system reference. Active mass: 1.00 g/monolith sample. Feed composition during adsorption: 100 ppm SO_2 and 7% O_2 in Ar. GHSV: 33 400 h^{-1}.

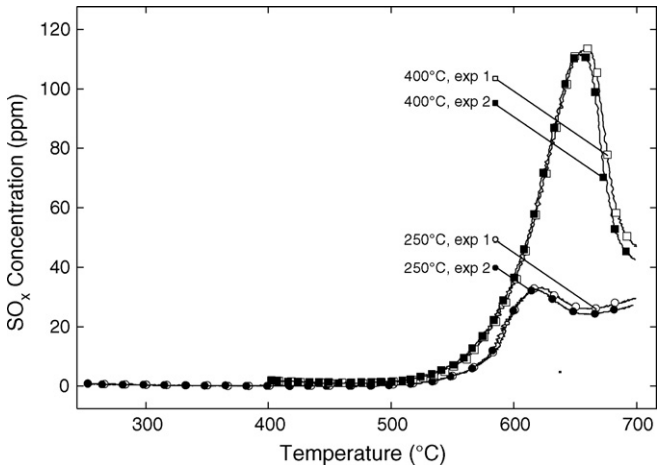

Fig. 6. SO_x signals from the desorption part of the repeated lean SO_2 adsorption and SO_x-TPD experiments performed with a 1 wt.% Pt/CeO_2 sample. The SO_2 adsorption temperature was alternated in the following sequence: 400, 250, 400 and 250 °C. Feed composition during the TPD: 7% O_2 in Ar. GHSV: 33 400 h^{-1}. Ramp rate: 10 °C/min.

(increased outlet SO_x concentration) can be observed between 550 and 700 °C with increasing Pt load of the sample. The same trend is observed for the SO_2 pre-exposed samples. However, comparing SO_x desorption from fresh and SO_2 pre-exposed samples with the same Pt loading generally shows that more SO_x is released from the SO_2 pre-exposed samples.

To investigate the influence of adsorption temperature on the SO_x storage and release capacity as well as the stability of the SO_x trap, repeated lean SO_x adsorption and TPD experiments were performed. The results from these experiments for the 1 wt.% Pt/CeO_2 sample are shown in Figs. 5 and 6. The experiments were performed with the same 1 wt.% Pt/CeO_2 sample used for the experiments shown in Figs. 3 and 4 as this sample already was exposed to large amounts of SO_2 at both 250 and 400 °C. The SO_2 adsorption was performed at two different temperatures following the sequence; 400, 250, 400 and 250 °C (with intermediate lean SO_x-TPD). The SO_x signals for the first and second SO_x adsorption and SO_x desorption coincide, revealing stable performance both at 250 and 400 °C. For lean SO_x adsorption, the outlet SO_x concentration is generally much lower when adsorption is performed at 400 °C as compared to at 250 °C. Considering the SO_x-TPD approximately twice as much SO_x are released after adsorption at 400 °C as compared to at 250 °C.

In Fig. 7, the amount of SO_x stored during the adsorption part of the experiments shown in Figs. 3 and 5 as well as the amount released during the regeneration part shown in Figs. 4 and 6 are summarised.

3.2. DRIFTS experiments

The results from the DRIFTS experiments where lean SO_x adsorption is performed at 250 °C for the CeO_2 and 5 wt.% Pt/CeO_2 samples and at 400 °C for the 5 wt.% Pt/CeO_2 sample are displayed in Fig. 8 whereas results from the corresponding experiments for the Al_2O_3 and 5 wt.% Pt/Al_2O_3 samples are shown in Fig. 9. The spectra presented in Figs. 8 and 9 are subtractions of two spectra where the reference spectra are recorded after the pre-treatment at the temperature to be measured. The lean SO_x adsorption for the CeO_2 sample at 250 °C results in several absorption bands between 800 and 1450 cm^{-1} (cf. Fig. 8a). After 5 min of SO_2 exposure, bands at 1365, 1325 (shoulder), 1215, 1175, 1100, 1000, 890 and 850 (shoulder) can be observed. Waqif et al. [15] have previously performed SO_2 adsorption studies using FTIR for both high and low surface area CeO_2 and assigned sharp bands between 1340 and 1400 cm^{-1} to surface sulfates and broad bands near 1160 cm^{-1} to bulk sulfates. The bands below 1050 cm^{-1} in the present study are probably due to weakly bound surface sulfites or hydrogen sulfites [15]. After further SO_2 exposure of the CeO_2 sample and in agreement with the results from the study by Waqif et al. [15], a second shoulder evolve around 1390 cm^{-1} in the surface sulfate region of the spectrum (cf. Fig. 8a). The broad band around 1175 cm^{-1} with a shoulder at 1215 cm^{-1} (attributed to bulk sulfates) is weak after 5 min of SO_2 exposure, however the intensity of the band increases during the SO_2 exposure. The positions of the bulk sulfate band and accompanying shoulder are

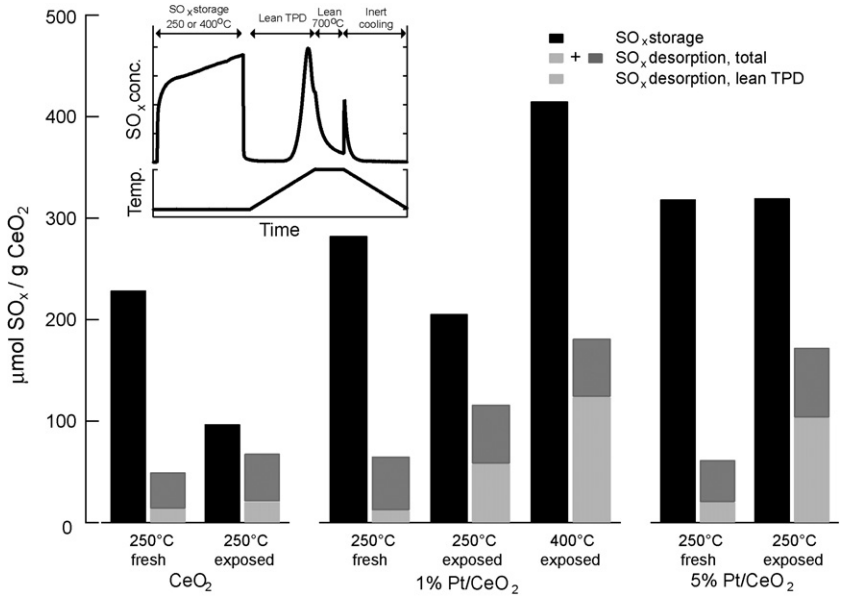

Fig. 7. Stored and released amount of SO_x for CeO_2-based SO_x traps calculated from the SO_x response during the SO_x adsorption and subsequent TPD experiments presented in Figs. 3–6. The total SO_x desorption is the sum of the release immediately after SO_2 has been switched off before starting the TPD-ramp, the release during the lean-TPD, the release when keeping the temperature constant at 700 °C under lean conditions and the release during the inert cooling ramp.

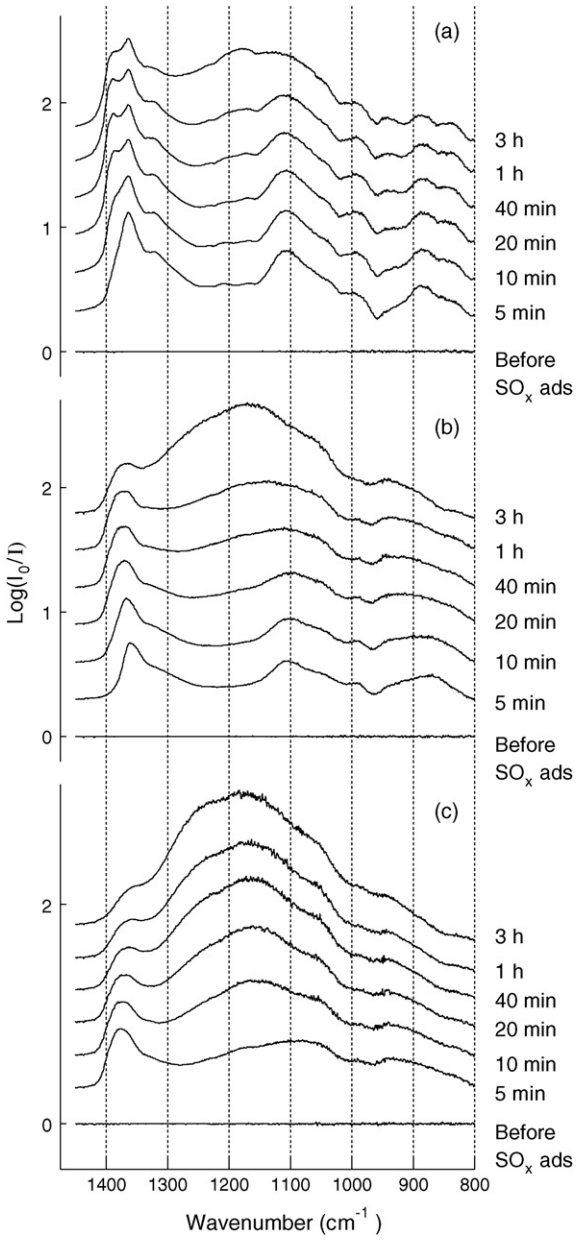

Fig. 8. DRIFTS results from lean SO_2 exposure of (a) CeO_2 at 250 °C, (b) 5 wt.% Pt/CeO_2 at 250 °C and (c) 5 wt.% Pt/CeO_2 at 400 °C. Feed composition during SO_2 exposure: 300 ppm SO_2 and 7% O_2 in Ar. Feed composition during recording of spectra: 7% O_2 in Ar. Total gas flow: 100 ml/min.

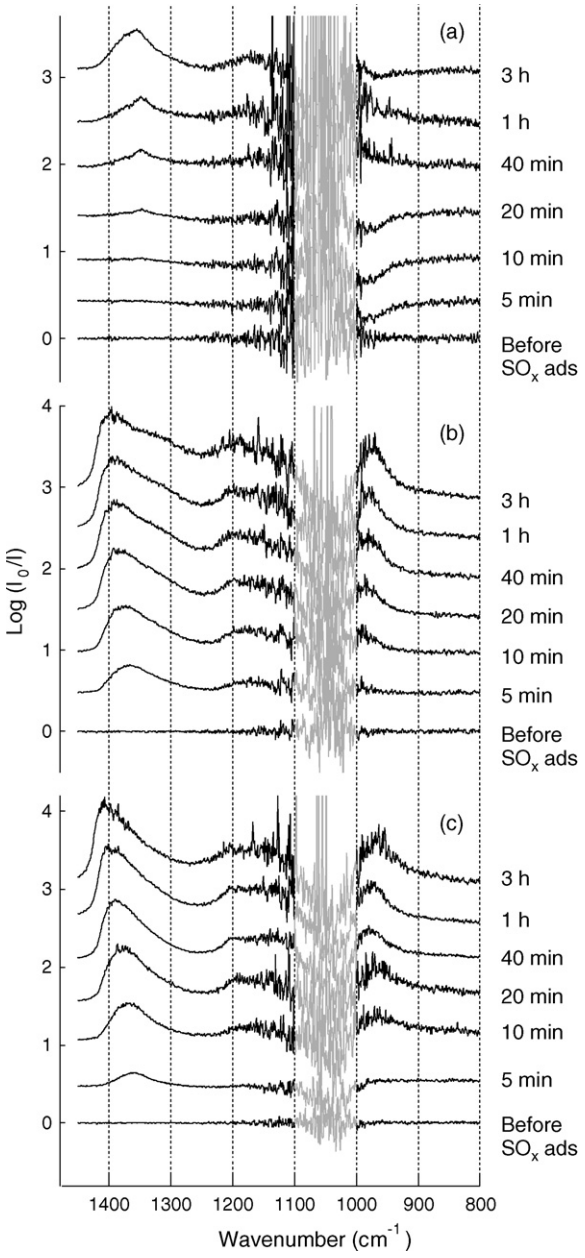

Fig. 9. DRIFTS results from lean SO_2 exposure of (a) Al_2O_3 at 250 °C, (b) 5 wt.% Pt/Al_2O_3 at 250 °C and (c) 5 wt.% Pt/Al_2O_3 at 400 °C. Feed composition during SO_2 exposure: 300 ppm SO_2 and 7% O_2 in Ar. Feed composition during recording of spectra: 7% O_2 in Ar. Total gas flow: 100 ml/min.

shifted during the SO_2 exposure and are finally positioned at 1180 and 1235 cm^{-1}, respectively, after 3 h.

The corresponding results for the Pt/CeO_2 sample (cf. Fig. 8b) show absorption bands in the same regions as for the CeO_2 sample, however, the bands are generally broader. In contrast to the surface sulfate band for the CeO_2 sample, the band around 1370 cm^{-1} for the Pt/CeO_2 sample is not shifted towards higher wavenumbers during the SO_2 exposure. Instead, this band becomes broader and the magnitude decreases slightly. The magnitude of the bulk sulfate bands (1180 and 1240 cm^{-1}) increases more rapidly for the Pt/CeO_2 sample as compared to the CeO_2 sample at 250 °C.

The increase of the adsorption temperature to 400 °C for the Pt/CeO_2 sample (cf. Fig. 8c) results in an even faster increase in magnitude of the bulk sulfate bands whereas the magnitude of the surface sulfate band formed after 5 min of SO_2 exposure decreases more rapidly than at 250 °C.

Lean SO_2 adsorption at 250 °C on the bare Al_2O_3 sample (cf. Fig. 9a) results in fewer adsorption bands between 800 and 1450 cm^{-1} as compared to the CeO_2 sample. Due to non-diluted samples, the infrared radiation is completely absorbed by Al_2O_3 between 1000 and 1100 cm^{-1} with the present experimental setup. After 20 min of SO_2 exposure, a weak band around 1350 cm^{-1} evolves which increases during the exposure and shifts slightly to higher wavenumbers around 1360 cm^{-1}. Saur et al. [20] have previously prepared surface sulfur species on Al_2O_3 and TiO_2 by various preparation routes. With FTIR spectroscopy, two accompanying bands at 1380 and 1045 cm^{-1} were assigned to surface sulfates on Al_2O_3. The band between 1350 and 1360 cm^{-1} in Fig. 9a originates most likely from surface sulfates on the Al_2O_3

sample. In addition to the band around 1360 cm^{-1}, a weak band at 1160 cm^{-1} evolves for the Al_2O_3 sample after approximately 1 h of SO_2 exposure. This band was not observed by Saur et al. [20]. However, Mitchell et al. [21] have reported formation of an absorption band at 1190 cm^{-1} after oxidising adsorbed SO_2 species on Al_2O_3. The different results obtained in these two studies may originate from different sample preparation procedures and experimental setups. The IR spectrum by Mitchell et al. is very similar to the spectrum of bulk aluminium sulfate. The weak band around 1160 cm^{-1} in Fig. 9a could therefore be due to bulk sulfates in the Al_2O_3 sample, analogous to the bulk sulfate band around 1180 cm^{-1} for CeO_2. However, in this study, the DRIFTS experiments with the Al_2O_3 samples are performed to verify that the results obtained from the flow-reactor experiments are not effects of the binder, Boehmite. Hence, the assignment of the controversial 1160 cm^{-1} band for the Al_2O_3 samples is beyond the scope of this study. When SO_x adsorption is performed at 250 °C for the Pt/Al_2O_3 sample (cf. Fig. 9b), absorption bands can be observed in the same regions as for the Al_2O_3 sample. However, the surface sulfate band is detected at slightly higher wavenumber, 1370 cm^{-1}, already after 5 min of SO_2 exposure and shifts to around 1400 cm^{-1} during the experiment. The broad band around 1160 cm^{-1} is also formed already after 5 min of SO_2 exposure and the magnitude of both this band and the surface sulfate band increases during the experiment. When SO_x adsorption is performed at 400 °C on the Pt/Al_2O_3 sample (cf. Fig. 9c) no significant difference can be seen as compared to adsorption at 250 °C on the same type of sample.

4. Discussion

Ceria is an interesting material for regenerable SO_x traps owing to its basic properties and mobile oxygen ions. The results from flow-reactor experiments with synthetic gas compositions in this study indicate that CeO_2 indeed is a suitable material for regenerable SO_x traps under lean conditions. Sulfur oxides are stored at temperatures between 200 and 500 °C and released slightly above 500 °C under lean conditions. In Fig. 1, lean SO_x adsorption for three different SO_x adsorbents is compared. Under these conditions, the Pt/CeO_2 and Pt/Al_2O_3 samples clearly show highest SO_x storage ability, i.e., slow increase in outlet SO_x concentration, as compared to the Pt/Al_2O_3:MgO and Al_2O_3:MgO samples. Note that the used inlet SO_2 concentration, 100 ppm, is considerably higher than expected for real lean exhausts. During the subsequent SO_x desorption (cf. Fig. 2), the Al_2O_3:MgO-based samples release SO_x already below 500 °C. Thus, these materials do not form sufficiently stable sulfur species to meet the specified requirements. The Al_2O_3 and CeO_2-based samples do not release any significant amounts of SO_x below 500 °C. At temperatures slightly above 500 °C the SO_x desorption rate is highest for the Pt/CeO_2 sample. It is also clear that addition of Pt to the CeO_2 sample enhances the rate of both SO_x storage and release. On the basis of these results, we focus the remaining discussion on ceria and the influence of Pt on the SO_x storage and release kinetics under lean conditions emphasising the analogies with NO_x storage and release in NO_x storage catalysts.

Bazin et al. [22] have previously reported similar SO_x adsorption capacity under lean conditions at 400 °C for CeO_2 samples with and without Pt as presented in this study. In contrast to the results reported by Bazin et al., our results show that at 250 °C the SO_x storage capacity of ceria samples under lean conditions is increased by including Pt on the samples, cf. Fig. 1. This is further emphasised when comparing the results for SO_x storage (cf. Figs. 3 and 7) for the different ceria samples, i.e., CeO_2, 1 wt.% Pt/CeO_2 and 5 wt.% Pt/CeO_2, clearly showing an increase in SO_x storage capacity with increased Pt content. The reason for this trend is most likely connected to the importance of the SO_2 oxidation kinetics over Pt and the subsequent adsorption on ceria as sulfates. This is analogous to NO oxidation which has shown to be crucial for efficient NO_x storage on BaO for NO_x storage catalysts [23,24]. Even though SO_3 is the thermodynamically stable compound under lean conditions in the temperature interval of interest, i.e., 200–500 °C, the formation of SO_3 is most likely kinetically limited in the lower temperature range. This is reflected by the low SO_x storage capacity for the pure ceria sample at 250 °C. However, when Pt is added to the sample, the SO_3 formation significantly increases and thus also the SO_x storage capacity. As ceria exhibits recognised dynamic redox behaviour [14] sulfates may form directly on ceria provided that the temperature is sufficiently high to overcome the activation barrier for this process. Thus, at elevated temperatures, sulfate formation on pure ceria may be sufficiently high to conceal additional effects of Pt on the SO_x storage kinetics. This most likely explains the difference between our measurements and the results reported by Bazin et al. where SO_x adsorption was performed at 400 °C.

The DRIFTS results from SO_x adsorption on CeO_2-based samples show several absorption bands between 500 and 1700 cm^{-1}. However, as the complete description of the origin of these bands is beyond the scope of the present study, we limit the discussion to the separation of surface and bulk sulfates. As the magnitude of the broad band around 1180 cm^{-1} with a shoulder at 1240 cm^{-1} increases more rapidly for the Pt/CeO_2 sample as compared to the CeO_2 sample at 250 °C, we may conclude that Pt increases the rate of bulk sulfate formation. The increased rate of bulk sulfate formation is most likely due to increased rate of surface sulfate formation. Besides the kinetic effects of SO_3 formation (i.e., higher SO_2 oxidation rate over Pt), the increased rate of sulfate formation could also be connected to Pt-assisted oxygen transfer, i.e., spill-over of oxygen, from platinum to ceria sites with adsorbed SO_2 in the close vicinity of the Pt crystallites. Independently of which route the surface sulfates are formed by, the formation will result in a considerable difference in sulfate concentration between the surface and bulk of ceria and thus a driving force for diffusion of sulfates into the bulk. The structure of ceria facilitates ion diffusion [14] and the exchange rate of ions between bulk and surface should be rather high. In this context it should be noted that the available surface area for SO_2 adsorption is similar for the CeO_2 and Pt/CeO_2 samples as confirmed by the N_2-physisorption measurements (cf. Table 1).

When considering regeneration under lean conditions of the ceria-based samples, the amount of SO_x released during the temperature programmed desorption increases with increased Pt loading (0–5 wt.% Pt) of the samples (cf. Figs. 4 and 7). Because more SO_x is stored during the adsorption part of the experiment on CeO_2 samples with higher Pt loading, it is not surprising that more SO_x also is released during the regeneration. The same trend is observed during the lean SO_x-TPD subsequent of adsorption at 250 and 400 °C for the 1 wt.% Pt/CeO_2 sample. A higher amount of SO_x is released after SO_x adsorption at 400 °C as compared to at 250 °C, as more SO_x is stored at 400 °C. However, it is also possible to see a shift in the temperature where the desorption starts related to the Pt content of the CeO_2 samples, especially for the fresh samples in Fig. 4, where the desorption of SO_x starts at 550 °C for the 5 wt.% Pt/CeO_2 sample and slightly above 600 °C for the CeO_2 sample. For the exposed samples, a shoulder on the desorption curve or even a desorption maximum below 700 °C can be observed for the Pt-containing samples (cf. Figs. 4 and 6) whereas such shoulder is absent for the CeO_2 samples below 700 °C. These observations indicate that the increased SO_x desorption from CeO_2 samples with higher Pt loading is not only due to the higher SO_x storage capacity of these samples. In analogy with NO_x storage catalysts [25], the

presence of Pt likely influences the release process of SO_x. As the sulfates appear to be fairly mobile in the sample, it is possible that reversed spill-over of sulfates from ceria sites close to Pt onto Pt sites can decrease the desorption temperature of these sulfur oxide species. The different SO_x release behaviour could also be owing to different adsorption sites available on the Pt-containing samples.

Comparison between the results for fresh and SO_2 pre-exposed CeO_2-based samples indicates that there are different SO_x adsorption sites available on the samples. During the adsorption part of the experiment (cf. Figs. 3, 5 and 7) the SO_x adsorption capacity is higher for the fresh CeO_2 and 1 wt.% Pt/CeO_2 samples as compared to the exposed samples whereas no difference between fresh and exposed sample can be seen for the 5 wt.% Pt/CeO_2 sample. During the regeneration, a higher amount SO_x is released from the exposed samples in all cases. The part of the total SO_x release which desorbs during the lean-TPD is also higher for the exposed samples in all cases and especially for the Pt-containing samples (cf. Fig. 7). From these results we conclude that not all storage sites on the CeO_2-based SO_x traps are possible to regenerate under lean conditions at below 700 °C. For the fresh sample, storage takes place on both regenerable and non-regenerable sites whereas for the SO_2 pre-exposed sample, the storage almost exclusively takes place on regenerable sites. Because bulk sulfate formation is more rapid at 400 °C as compared to at 250 °C, it could be assumed that during the first temperature increase the formed surface sulfates migrate into the ceria bulk instead of being released from the sample. Therefore, the release of SO_x is low during the first regeneration. During the saturation step where the samples are exposed to high amounts of SO_2 at 250 and 400 °C these bulk sites will probably be saturated or almost saturated. During the second regeneration, more SO_x is released as it is no longer possible for the sulfates to diffuse into the bulk during the temperature increase. Furthermore, the difference between SO_x storage capacity for fresh and pre-exposed sample is low or negligible when the Pt content of the sample is increased. The release around 600 °C, on the other hand, changes most for the samples with high Pt content. When increasing the Pt loading of the sample, the Pt/CeO_2 contact area will most probably also increase. From these results it can be assumed that SO_x storage takes place more rapidly on storage sites close to Pt and that these storage sites are more easily regenerated than the corresponding sites located far away from Pt. Therefore, when increasing the Pt loading of the CeO_2 samples, the number of regenerable SO_x storage sites will also increase.

5. Concluding remarks

Materials for regenerable SO_x traps with the ability to store and release SO_x under lean conditions but at different temperature intervals were investigated. Among the studied materials, Pt/CeO_2 was recognised to be most promising. Under lean conditions, Pt/CeO_2 shows the highest SO_x storage ability at 250 °C and most efficient release around 600 °C. It is found that the lean SO_x adsorption capacity at 250 °C and subsequent release in the temperature interval 500–700 °C increases with increased Pt loading (0, 1 and 5 wt.% Pt). Results from DRIFTS experiments reveal that SO_2 adsorption on CeO_2 samples under lean conditions proceeds via the formation of surface and bulk sulfates. The rate of bulk sulfate formation is higher for the Pt-impregnated CeO_2 sample. Increasing the adsorption temperature, from 250 to 400 °C resulted in an increased amount of adsorbed SO_x for the 1 wt.% Pt/CeO_2 sample. This is probably owing to faster SO_2 oxidation kinetics at 400 °C and that the SO_3 formation facilitates storage on CeO_2. An increased adsorption temperature from 250 to 400 °C is also found to yield more rapid bulk sulfate formation for the Pt/CeO_2 sample.

Moreover, SO_x adsorption and regeneration of fresh and SO_2 pre-exposed samples were compared. Generally, a lower amount of SO_x can be stored on the pre-exposed samples but for the 5 wt.% Pt/CeO_2 sample, no significant difference between fresh and pre-exposed samples can be observed. During the subsequent regeneration, more SO_x are released from the exposed samples in all cases. These results indicate that some of the storage sites on the CeO_2-based samples are not possible to regenerate at 700 °C or below under lean conditions. During the pre-exposure, the SO_x storage capacity decreases less and the SO_x release increases most for the samples with higher Pt loading. This indicates that Pt increases the number of regenerable sites on the SO_x trap or that Pt increases the formation of a certain sulfur species that both forms faster during adsorption conditions and releases faster during desorption conditions.

Acknowledgements

This work has been performed within the GREEN-project which is financially supported by the European Commission FP6 Programme (Contract no: FP6-516195), and partly within the Competence Centre for Catalysis which is financially supported by Chalmers University of Technology, the Swedish Energy Agency and the member companies: AB Volvo, Volvo Car Corporation, Scania CV AB, GM Powertrain Sweden AB, Haldor Topsøe A/S and The Swedish Space Corporation.

Appendix A

A.1. Continuous monitoring of total SO_x concentration in a lean gas flow

To evaluate the performance of model SO_x traps in a flow-reactor setup, continuous monitoring of total SO_x concentration in the gas flow is necessary. A method facilitating analysis of the total SO_x concentration in a lean gas flow using a SO_2 analyser has previously been reported by D. McLaughlin et al. at the Taylor conference in Belfast 2004. Following this method with only minor modifications, the gas flow was passed over an oxidation catalyst before introduced to the SO_2 analyser (non-dispersive IR, Maihak

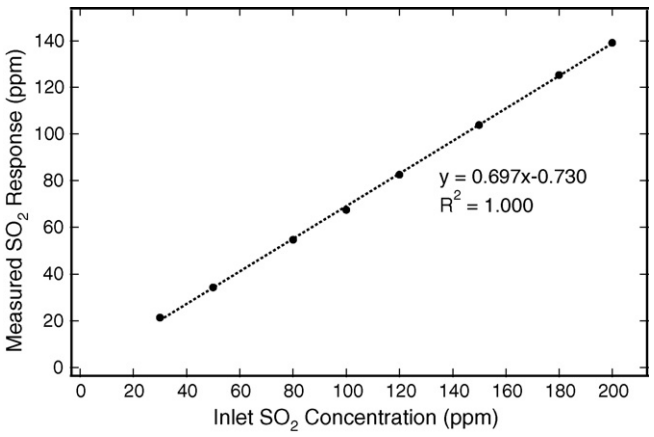

Fig. A.1. Measured SO_2 response during calibration with various inlet SO_2 concentrations. The gas flow is passed over an oxidation catalyst heated to 675 °C before introduced to the SO_2 analyser. Feed composition: 30, 50, 80, 100, 120, 150, 180 or 200 ppm SO_2 and 7% O_2 in Ar.

UNOR 610). The oxidation catalyst (Pt/SiO_2) was heated to 675 °C which is the equilibrium temperature for the composition 50% SO_2/50% SO_3 in oxygen excess. Due to instrumental cross sensitivity for SO_2 and SO_3, about 70% of the total amount of SO_x was detected as SO_2 with the present experimental setup (cf. Fig. A.1). From the measured SO_2 response, the total SO_x concentration was finally estimated. In order to ensure the performance of the oxidation catalyst and the IR instrument, calibration with 100 ppm SO_2 and 7% O_2 in Ar was performed before as well as after each experiment.

References

[1] S. Matsumoto, Cattech 4 (2001) 102–109.
[2] N. Takahashi, H. Shinjoh, T. Iijima, T. Suzuki, K. Yamazaki, K. Yokota, H. Suzuki, N. Miyoshi, S. Matsumoto, T. Tanizawa, T. Tanaka, S.-s. Tateishi, K. Kasahara, Catal. Today 27 (1996) 63–69.
[3] A. Amberntsson, B. Westerberg, P. Engström, E. Fridell, M. Skoglundh, Studi. Surf. Sci. Catal. 126 (1999) 317–324.
[4] C. Sedlmair, K. Seshan, A. Jentys, J.A. Lercher, Cataly. Today 75 (2002) 413–419.
[5] J. Dawody, M. Skoglundh, L. Olsson, E. Fridell, J. Catal. 234 (2005) 206–218.
[6] S. Matsumoto, Y. Ikeda, H. Suzuki, M. Ogai, N. Miyoshi, Appl. Catal. B: Environ. 25 (2000) 115–124.
[7] G. Centi, G. Fornasari, C. Gobbi, M. Livi, F. Trifiro, A. Vaccari, Catal. Today 73 (2002) 287–296.
[8] G. Fornasari, R. Glöckler, M. Livi, A. Vaccari, Appl. Clay Sci. 29 (2005) 258–266.
[9] L. Limousy, H. Mahzoul, J.F. Brilhac, P. Gilot, F. Garin, G. Maire, Appl. Catal., B: Environ. 42 (2003) 237–249.
[10] H. Dathe, A. Jentys, J.A. Lercher, Phys. Chem. Chem. Phys. 7 (2005) 1283–1292.
[11] L. Li, D.L. King, Ind. Eng. Chem. Res. 44 (2005) 7388–7397.
[12] K. Tikhomirov, O. Kröcher, M. Elsener, M. Widmer, A. Wokaun, Appl. Catal., B: Environ. 67 (2006) 160–167.
[13] A. Amberntsson, M. Skoglundh, S. Ljungström, E. Fridell, J. Catal. 217 (2003) 253–263.
[14] A. Trovarelli, Catalysis by Ceria and Related Materials, Catalytic Science Series, Imperial College Press, London, 2005.
[15] M. Waqif, P. Bazin, O. Saur, J.C. Lavalley, G. Blanchard, O. Touret, Appl. Catal., B: Environ. 11 (1997) 193–205.
[16] A.E. Palomares, J.M. López-Nieto, F.J. Lázaro, A. López, A. Corma, Appl. Catal., B: Environ. 20 (1999) 257–266.
[17] S. Brunauer, P.H. Emmett, E. Teller, J. Am. Chem. Soc. 60 (1938) 309–319.
[18] J. Dawody, M. Skoglundh, S. Wall, E. Fridell, J. Mol. Catal. A: Chem. 225 (2005) 259–269.
[19] D. McLaughlin, F. Meunier, J.P. Breen, R. Burch (unpublished).
[20] O. Saur, M. Bensitel, A.B.M. Saad, J.C. Lavalley, C.P. Tripp, B.A. Morrow, J. Catal. 99 (1986) 104–110.
[21] M.B. Mitchell, V.N. Sheinker, M.G. White, J. Phys. Chem. 100 (1996) 7550–7557.
[22] P. Bazin, O. Saur, J.C. Lavalley, G. Blanchard, V. Visciglio, O. Touret, Appl. Catal., B: Environ. 13 (1997) 265–274.
[23] E. Fridell, M. Skoglundh, B. Westerberg, S. Johansson, G. Smedler, J. Catal. 183 (1999) 196–209.
[24] L. Olsson, H. Persson, E. Fridell, M. Skoglundh, B. Andersson, J. Phys. Chem. B 105 (2001) 6895–6906.
[25] I. Nova, L. Lietti, L. Castoldi, E. Tronconi, P. Forzatti, J. Catal. 239 (2006) 244–254.